CORA Cork Open Research Archive
Cartlann Taighde Oscailte Chorcaí

Title	Time- and momentum-resolved probe of heat transport in photo-excited bismuth
Authors	Chen, J.;Trigo, M.;Fahy, Stephen B.;Murray, Éamonn D.;Sheu, Y. M.;Graber, T.;Henning, R.;Chien, Y. J.;Uher, C.;Reis, D. A.
Publication date	2013
Original Citation	Chen, J., Trigo, M., Fahy, S., Murray, É. D., Sheu, Y. M., Graber, T., Henning, R., Chien, Y. J., Uher, C. and Reis, D. A. (2013) 'Time- and momentum-resolved probe of heat transport in photo-excited bismuth', Applied Physics Letters, 102(18), pp. 181903. doi: 10.1063/1.4804291
Type of publication	Article (peer-reviewed)
Link to publisher's version	http://dx.doi.org/10.1063/1.4804291 - 10.1063/1.4804291
Rights	© 2013 AIP Publishing LLC..This article may be downloaded for personal use only. Any other use requires prior permission of the author and AIP Publishing. The following article appeared in Chen, J., Trigo, M., Fahy, S., Murray, É. D., Sheu, Y. M., Graber, T., Henning, R., Chien, Y. J., Uher, C. and Reis, D. A. (2013) 'Time- and momentum-resolved probe of heat transport in photo-excited bismuth', Applied Physics Letters, 102(18), pp. 181903 and may be found at http://dx.doi.org/10.1063/1.4804291
Download date	2026-11-15 11:44:31
Item downloaded from	https://hdl.handle.net/10468/4284

UCC
University College Cork, Ireland
Coláiste na hOllscoile Corcaigh

Time- and momentum-resolved probe of heat transport in photo-excited bismuth

J. Chen' , M. Trigo, S. Fahy, É. D. Murray, Y. M. Sheu, T. Graber, R. Henning, Y. J. Chien' , C. Uher, and D. A. Reis

Citation: Appl. Phys. Lett. **102**, 181903 (2013); doi: 10.1063/1.4804291
View online: http://dx.doi.org/10.1063/1.4804291
View Table of Contents: http://aip.scitation.org/toc/apl/102/18
Published by the American Institute of Physics



Time- and momentum-resolved probe of heat transport in photo-excited bismuth

J. Chen,[1,2,a)] M. Trigo,[1] S. Fahy,[3] É. D. Murray,[4] Y. M. Sheu,[5] T. Graber,[6] R. Henning,[6] Y. J. Chien,[7,b)] C. Uher,[7] and D. A. Reis[1,2]
[1]*PULSE Institute, SLAC National Accelerator Laboratory, Menlo Park, California 94025, USA*
[2]*Department of Photon Science and Applied Physics, Stanford University, Stanford, California 94305, USA*
[3]*Department of Physics, University College Cork, Cork, Ireland*
[4]*Department of Chemistry, University of California, Davis, California 95616, USA*
[5]*Center for Integrated Nanotechnologies, MS K771, Los Alamos National Laboratory, Los Alamos, New Mexico 87545, USA*
[6]*The Center for Advanced Radiation Sources, University of Chicago, Chicago, Illinois 60637, USA*
[7]*Department of Physics, University of Michigan, Ann Arbor, Michigan 48109-1040, USA*

(Received 24 January 2013; accepted 24 April 2013; published online 7 May 2013)

We use time- and momentum-resolved x-ray scattering to study thermalization in a photo-excited thin single crystal bismuth film on sapphire. The time-resolved changes of the diffuse scattering show primarily a quasi-thermal phonon distribution that is established in $\lesssim$100 ps and that follows the time-scale of thermal transport. Ultrafast melting measurements under high laser excitation show that epitaxial regrowth of the liquid phase occurs on the time-scale of thermal transport across the bismuth-sapphire interface. © *2013 AIP Publishing LLC*. [http://dx.doi.org/10.1063/1.4804291]

The dynamics of photo-excited semi-metallic bismuth are determined by the strong interactions between the electronic and lattice degrees of freedom.[1] In particular, there has been sustained interest in the coupling between the photo-excited carriers and the zone-center longitudinal (A_{1g}) optical phonon,[2,3] as it relates directly to the magnitude of the Peierls distortion. Through ultrafast optical reflectivity[4–7] as well as x-ray diffraction experiments,[8–10] the mode is known to soften with increasing carrier density concomitant with an increase in equilibrium distance between nearest neighbors as the system is driven towards a more symmetric state. At the same time, the A_{1g} lifetime decreases. As the above experiments are sensitive to the average structure, little to no information is gained on the dynamics of modes that carry nonzero momentum. Previously, we have shown that time resolved x-ray diffuse scattering can be used to follow the evolution of the non-equilibrium phonon distribution throughout the Brillouin zone.[11] In those experiments, on the polar semiconductors InP and InSb, we found a surprisingly long-lived non-thermal state that involved the delayed emission of high frequency, high wavevector transverse acoustic modes. Here, we use time-resolved diffuse scattering to study the structural dynamics of photo-excited bismuth excited both above and below its melting threshold with momentum resolution spanning the entire Brillouin zone. Below the melting threshold, we find that the phonon population primarily follows a quasi-equilibrium thermal distribution that evolves on the time-scale of thermal transport. Above the single-shot melting threshold, we find that the film regrows epitaxially also on the time-scale of thermal transport.

The experiments are performed at Sector 14 (BioCARS)[12] of the Advanced Photon Source (APS) at Argonne National Laboratory. The experimental setup is similar to that described by Trigo *et al.*[11] We use x rays with 13 keV photon energy and ~100 ps pulse width, and a laser with 640 nm wavelength and ~1 ps pulse duration. The sample is a single crystal Bi thin film with thickness of ~250 nm epitaxially grown on a sapphire substrate with the c-axis along the surface normal. The laser is incident on the sample surface close to normal incidence, and the x-ray beam was incident at a grazing angle of 1.5°. Each x-ray pulse contains $\sim 10^{10}$ photons focused to a spot of 0.07×2.6 mm^2 on the sample. We estimate that the incident laser fluence was ~1 mJ/cm^2 when operating below and 5–30 mJ/cm^2 when operating above the melting threshold. A large area detector (MarCCD 165 mm diameter) placed 75 mm behind the sample collects the x rays with scattering angles of up to $2\theta \sim 48°$. All the measurements shown in this paper were taken at room temperature.

Figures 1–3 are based on measurements whose pump laser fluence is below the melting threshold at a repetition rate of 41 Hz. Fig. 1(a) shows a static (with no laser illumination) x-ray diffuse scattering image of Bi. The scattered intensity has contributions from diffuse scattering from the thermally excited phonons in addition to crystal-surface truncation rods[13] and a background due, for example, to static disorder, air scattering, and Compton scattering. Fig. 1(b) shows the simulated image of first order thermal diffuse scattering (TDS) for the same conditions as Fig. 1(a) including crystal orientation and x-ray energy. We obtain the eigenvectors and frequencies of the normal modes corresponding to the 6 phonon branches from first-principles calculations.[14,15] The technical details (convergence parameters, etc.) for the calculations are the same as those used by Murray *et al.*[1]

In thermal equilibrium, the intensity of one-phonon scattering at momentum transfer $\vec{Q}$ has contributions from the various modes of reduced wave vector $\vec{q}$ and frequency $\omega_{\mathbf{q},j}$ and is given by[11,16–18]

a)chenjian@slac.stanford.edu
b)Current address: AU Optronics Corporation, 1 JhongKe Rd., Central Taiwan Science Park, Taichung 40763, Taiwan.

 © 2013 AIP Publishing LLC

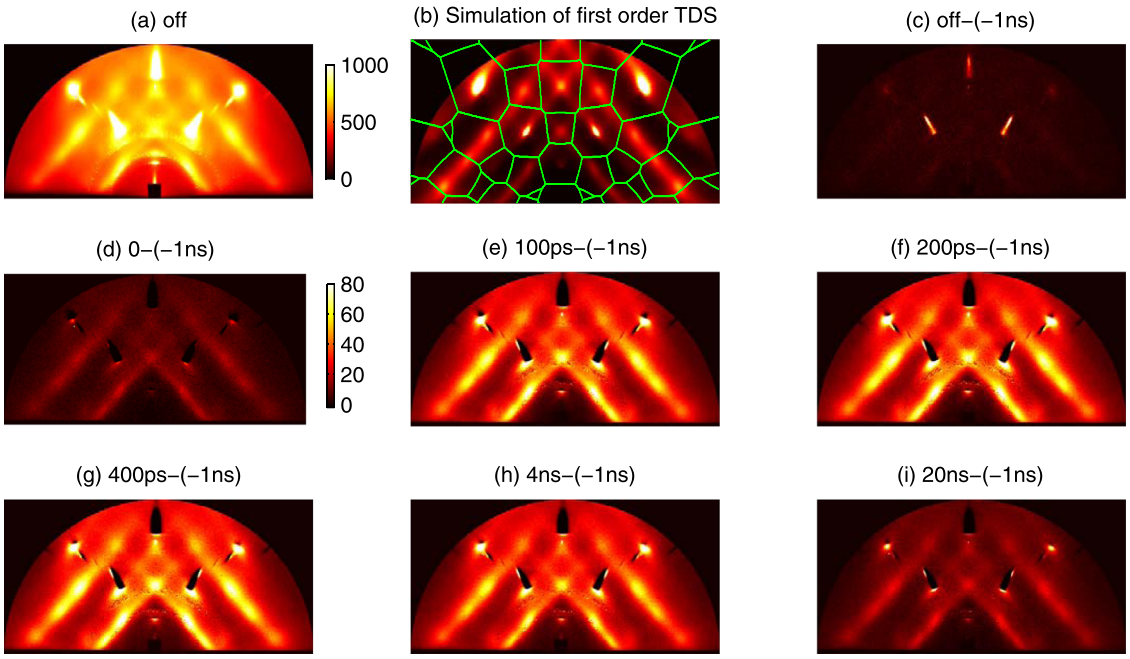


FIG. 1. (a) Room temperature TDS images of Bi at 13 keV oriented with (11–2) nearly parallel to the x-ray direction (grazing angle = 1.5°) with no laser illumination. (b) Calculated first order TDS, on top of which displayed the Brillouin zone boundaries. (c) Difference between laser-off and laser-late frame for comparison. (d)-(i) Differences between a few laser-early frames and laser-late frame, $I(t_i) - I(t < 0)$, showing the evolution of phonon distribution. ((c)-(i) use the same scale.)

$$I_1(\mathbf{Q};T) = \frac{\hbar N I_e}{2} \sum_j \frac{1}{\omega_{\mathbf{q},j}} \coth\left(\frac{\hbar\omega_{\mathbf{q},j}}{2k_B T}\right) |F_j(\mathbf{Q})|^2, \qquad (1)$$

where N is the number of unit cells, I_e is the scattering intensity from a single electron, and $F_j(\mathbf{Q})$ is the one-phonon structure factor, which is proportional to projection of the phonon polarization on the scattering vector.[18] The close similarities between Figures 1(a) and 1(b) give us confidence that away from the Bragg rods, the first order diffuse component contributes a significant fraction of the scattered intensity. Thus to a good approximation, time-resolved difference images between laser excited ($I(\mathbf{Q}, t > 0)$) and unexcited ($I(\mathbf{Q}, t < 0)$) images give a direct measure of the time-dependent changes in phonon occupation as a function of $\mathbf{Q}$ and delay t following laser excitation.

Figs. 1(d)–1(i) show $I(\mathbf{Q}, t) - I(\mathbf{Q}, t = -1\ \text{ns})$ for a few illustrative time delays. Following laser excitation, the scattering first increases for several hundred picoseconds, then decreases after a few nanoseconds, and eventually returns to equilibrium, in qualitative agreement with Trigo *et al.*[11] on InP and InSb. Figure 1(c) displays little difference between no laser excitation ("laser-off" image, Fig. 1(a)) and the x-ray pulse arriving 1 ns before laser excitation ("laser-late image," $I(\mathbf{Q}, t = -1\ \text{ns})$) showing that the sample returns to equilibrium between pulses.

In Fig. 2(a), we plot the time average of the difference data which closely resembles the calculated equilibrium diffuse scattering image in Fig. 1(b), showing that within our temporal resolution the scattering associated with the

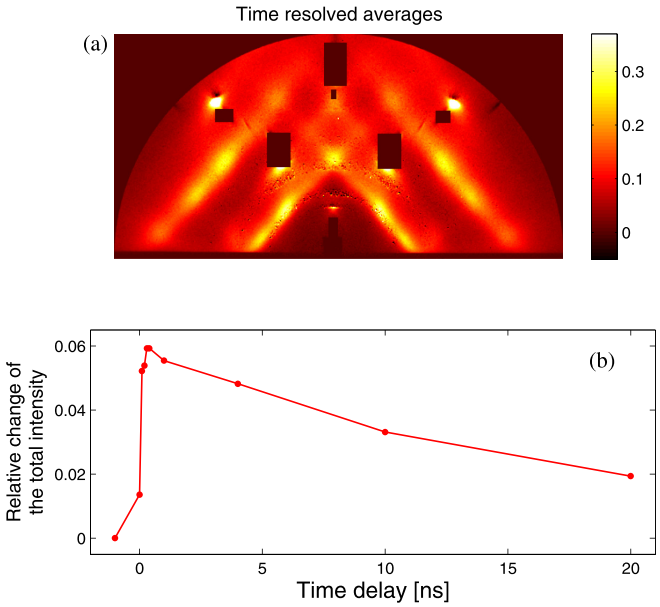


FIG. 2. Averages of the difference data. (a) Time averaged image (normalized), in which each pixel is averaged over all the time delays; and (b) relative change of the pixel averaged data to the static image. In each case, regions around the Bragg rods were masked out.

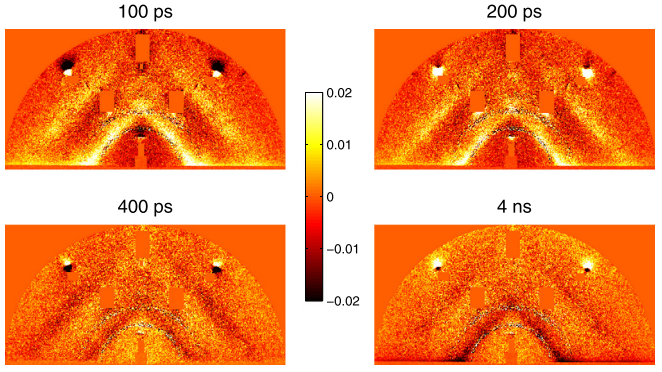


FIG. 3. Variation of the difference-images relative to the average for selected time delays. These figures are scaled by the normalization factor used for Fig. 2(a), so that we can compare their amplitudes.

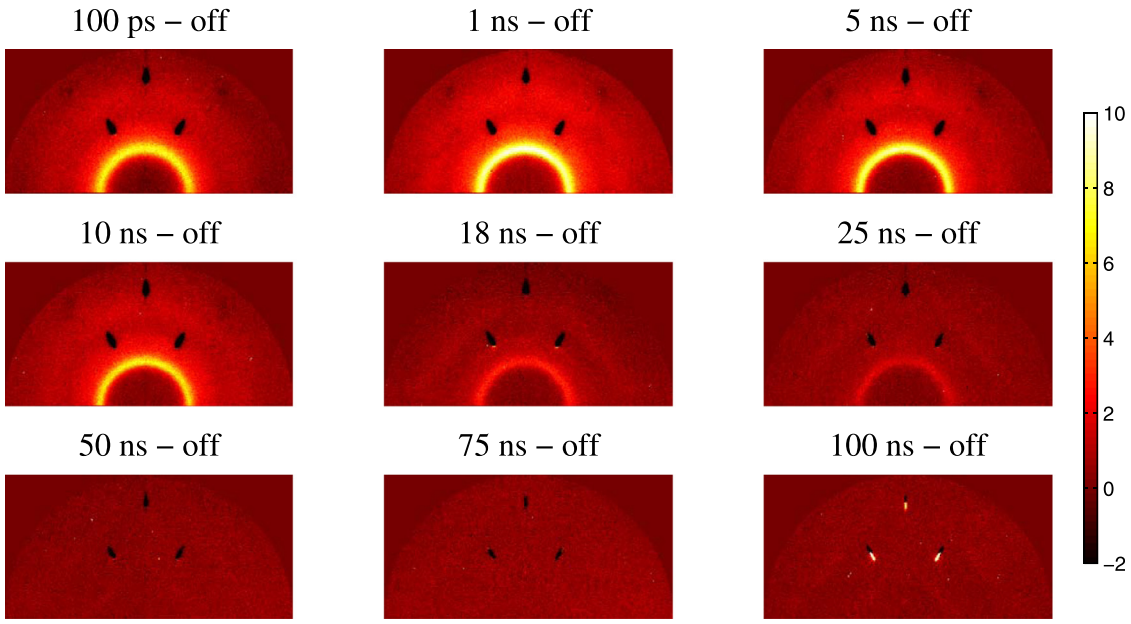


FIG. 4. Diffuse scattering images with laser on at different time delays minus images with laser off, i.e., $I(t_i) - I(\text{off})$, from our quasi-single-shot melting measurement. Each image is averaged over 5 pulses on the same sample spot, and different delay images are taken on different spots.

laser-excited bismuth is similar to what we would expect for a thermally excited sample at increased temperature when the modes are classically occupied (as in the case of Bi at room temperature). The corresponding time dependence of the average is shown in Fig. 2(b) and consists of a sharp increase followed by a decay with ∼10 ns time-constant, suggesting the time-resolved evolution corresponds to lattice heating followed by cooling due to thermal transport. The x-ray penetration depth at this angle is ∼400 nm, which is thicker than the Bi film which itself is thicker than the laser penetration depth, and thus we measure an average over the entire film thickness. Using a combination of time-resolved x-ray diffraction, Sheu *et al.*[19] determined that thermal transport following laser excitation in these films is dominated at early times by thermal diffusion in the film and on the nanosecond time-scale by the Kapitza conductance between the Bi and sapphire. Using the Kapitza conductance measured by Sheu *et al.*,[19] we obtain a time constant of cooling of ∼15.4 ns, in good agreement with our observation.

The maximum change of ∼6% in Fig. 2(b) corresponds to about 18 K temperature rise, averaged over the thickness of the sample, assuming all modes are thermally occupied and that the laser-off data are dominated by TDS. To see if there are substantial non-thermal contributions to the data, we calculated the residue of the image at various time-delays after subtracting the average, as shown in Fig. 3. The residue shows clear structure above the statistical noise. Nonetheless, the differences are small relative to the average, and we could not determine whether there is a significant contribution due to non-equilibrium phonons or lattice strain.

Under the same geometry as above, we increased the laser fluence to above melting threshold. Earlier ultrafast electron diffraction experiments[20] have studied the initial steps of Bi melting over the first few ps. We lack the temporal resolution to compare with these results. Instead, we concentrate on the cooling dynamics. Fig. 4 shows the time-resolved diffuse scattering image, similar to Figs. 1(d)–1(i) for this laser fluence. Each image is averaged over 5 pulses on the same sample spot, and different delay images are taken on different spots. There are no obvious laser-induced damages on the sample within 5 pulses of illumination, so our method is essentially the same as the single shot measurements. Not shown, after 5 shots we start to see permanent damage in the form of polycrystalline rings. We see from Fig. 4 that a liquid ring appears instantaneously (within our 100 ps resolution) upon strong laser illumination. The liquid-ring becomes strongest around 1 ns, presumably when the maximum amount of Bi is melted, and persists for ∼10 ns, after which it starts to fade and eventually disappears at ∼50 ns, showing epitaxial regrowth of Bi single crystal and the recurrence of the long-range order. This indicates the laser-induced liquid phase lasts for a similar time scale of that shown in Fig. 2(b), which suggests that the recrystallization of Bi is limited by the heat flow across the interface.

In conclusion, we find that the photoinduced evolution of diffuse scattering in single crystal Bi films is dominated by the thermal quasi-equilibrium change in phonon population, whose time scale agrees with the characteristic time of Kapitza conductance across the Bi/sapphire interface. Whereas laser-induced melting of Bi results in a liquid phase that lasts for a similar thermal time scale during which Bi grows back epitaxially into a single crystal state.

J.C., M.T., and D.A.R. acknowledge support from the U.S. Department of Energy office of Basic Energy Science through the Division of Materials Sciences and Engineering under Contract No. DE-AC02-76SF00515. S.F. acknowledges support from the Science Foundation Ireland. Use of the BioCARS Sector 14 was supported by grants from the National Center for Research Resources (5P41RR007707) and the National Institute of General Medical Sciences (8P41GM103543) from the National Institutes of Health. Use of the Advanced Photon Source, an Office of Science User Facility operated for the U.S. Department of Energy

(DOE) Office of Science by Argonne National Laboratory, was supported by the U.S. DOE under Contract No. DE-AC02-06CH11357. Time-resolved set-up at Sector 14 was funded in part through a collaboration with Philip Anfinrud (NIH/NIDDK). Single crystalline films of Bi were grown at the University of Michigan with the support of the Center for Solar and Thermal Energy Conversion, an Energy Frontier Research Center funded by the U.S. Department of Energy, Office of Science, Office of Basic Energy Sciences under Award No. DE-SC0000957.

[1]E. D. Murray, S. Fahy, D. Prendergast, T. Ogitsu, D. M. Fritz, and D. A. Reis, Phys. Rev. B **75**, 184301 (2007).
[2]J. J. Li, J. Chen, D. A. Reis, S. Fahy, and R. Merlin, Phys. Rev. Lett. **110**, 047401 (2013).
[3]Y. M. Sheu, Y. J. Chien, C. Uher, S. Fahy, and D. A. Reis, Phys. Rev. B **87**, 075429 (2013).
[4]T. K. Cheng, S. D. Brorson, A. S. Kazeroonian, J. S. Moodera, G. Dresselhaus, M. S. Dresselhaus, and E. P. Ippen, Appl. Phys. Lett. **57**, 1004 (1990).
[5]M. F. DeCamp, D. A. Reis, P. H. Bucksbaum, and R. Merlin, Phys. Rev. B **64**, 092301 (2001).
[6]M. Hase, M. Kitajima, S.-i. Nakashima, and K. Mizoguchi, Phys. Rev. Lett. **88**, 067401 (2002).
[7]E. D. Murray, D. M. Fritz, J. K. Wahlstrand, S. Fahy, and D. A. Reis, Phys. Rev. B **72**, 060301 (2005).
[8]K. Sokolowski-Tinten, C. Blome, J. Blums, A. Cavalleri, C. Dietrich, A. Tarasevitch, I. Uschmann, E. Forster, M. Kammler, M. H. von Hoegen, and D. von der Linde, Nature **422**, 287 (2003).
[9]D. M. Fritz, D. A. Reis, B. Adams, R. A. Akre, J. Arthur, C. Blome, P. H. Bucksbaum, A. L. Cavalieri, S. Engemann, S. Fahy, R. W. Falcone, P. H. Fuoss, K. J. Gaffney, M. J. George, J. Hajdu, M. P. Hertlein, P. B. Hillyard, M. H. von Hoegen, M. Kammler, J. Kaspar, R. Kienberger, P. Krejcik, S. H. Lee, A. M. Lindenberg, B. McFarland, D. Meyer, T. Montagne, D. Murray, A. J. Nelson, M. Nicoul, R. Pahl, J. Rudati, H. Schlarb, D. P. Siddons, K. Sokolowski-Tinten, T. Tschentscher, D. von der Linde, and J. B. Hastings, Science **315**, 633 (2007).
[10]S. L. Johnson, P. Beaud, E. Vorobeva, C. J. Milne, D. Murray, S. Fahy, and G. Ingold, Phys. Rev. Lett. **102**, 175503 (2009).
[11]M. Trigo, J. Chen, V. H. Vishwanath, Y. M. Sheu, T. Graber, R. Henning, and D. A. Reis, Phys. Rev. B **82**, 235205 (2010).
[12]T. Graber, S. Anderson, H. Brewer, Y.-S. Chen, H. S. Cho, N. Dashdorj, R. W. Henning, I. Kosheleva, G. Macha, M. Meron, R. Pahl, Z. Ren, S. Ruan, F. Schotte, V. Srajer, P. J. Viccaro, F. Westferro, P. Anfinrudb, and K. Moffata, J. Synchrotron Radiat. **18**, 658 (2011).
[13]I. K. Robinson, Phys. Rev. B **33**, 3830 (1986).
[14]S. Baroni, S. de Gironcoli, A. Dal Corso, and P. Giannozzi, Rev. Mod. Phys. **73**, 515 (2001).
[15]X. Gonze and C. Lee, Phys. Rev. B **55**, 10355 (1997).
[16]R. W. James, *The Optical Principles of the Diffraction of X Rays* (Ox Bow Press, 1982).
[17]B. Warren, *X-Ray Diffraction*, Dover Books on Physics (Dover Publications, 1990).
[18]R. Xu and T. C. Chiang, Z. Kristallogr. **220**, 1009 (2005).
[19]Y. Sheu, M. Trigo, Y. Chien, C. Uher, D. Arms, E. Peterson, D. Walko, E. Landahl, J. Chen, S. Ghimire, and D. Reis, Solid State Commun. **151**, 826 (2011).
[20]G. Sciaini, M. Harb, S. G. Kruglik, T. Payer, C. T. Hebeisen, F.-J. M. zu Heringdorf, M. Yamaguchi, M. H. von Hoegen, R. Ernstorfer, and R. J. D. Miller, Nature **458**, 56 (2009).